**Proceedings of the ASME 2020
International Design Engineering Technical Conferences
and Computers and Information in Engineering Conference
IDETC/CIE2020
August 17-19, 2020, Virtual, Online**

DETC2020-22349

A NOVEL BI-STABLE PIEZOELECTRIC ENERGY HARVESTER INSPIRED BY THE VENUS FLYTRAP

Feng Qian, Lei Zuo*
Department of Mechanical Engineering
Virginia Tech
Blacksburg, VA 24061

ABSTRACT

This paper studies the nonlinear dynamics and energy harvesting performance of a novel bi-stable piezoelectric energy harvester inspired by the rapid shape transition of the Venus flytrap leaves. The harvester is composed of a piezoelectric MFC transducer, a tip mass, and two sub-beams. The two sub-beams are akin to the bidirectionally curved Venus flytrap leaves that could rapidly snap- through from the open state to the closed state. To realize the bistability of the Venus flytrap leaves induced by the stored potential energy, an in-plane pre-displacement constraint is applied to the free ends of the sub-beams. The pre-displacement constraint leads to bending and twisting deformations and creates the potential energy in the harvester. The bio-inspired design is introduced in detail and a prototype is fabricated to validate the conceptual design. The nonlinear dynamics of the bio-inspired bi-stable piezoelectric energy harvester is investigated under base acceleration excitations. Results show that the sub-beams of the harvester experience more complicated local vibrations containing broadband high-frequency components as the snap-through motion happens. The energy harvesting performance of the harvester is evaluated at different excitation levels. The broadband energy harvesting is achieved at higher excitation levels and an average power output of 0.193 mW is attained under the excitation of 10 Hz and 4.0 g.

*Corresponding author: leizuo@vt.edu.

INTRODUCTION

The worldwide fossil energy crisis and the resultant environmental pollution problems have greatly motivated the research on alternative clean and renewable energy sources. Energy harvesting techniques that could effectively convert waste ambient energy in different forms into usable electricity has received increasing attention with the rapid development of wireless sensors and low-power electronics. The linear piezoelectric cantilever is one of the most widely studied energy transduction devices realizing mechanical-to-electrical energy conversion based on the direct piezoelectric effect [1]. However, linear piezoelectric energy harvesters are condemned for the problem of the narrow frequency bandwidth, which leads to the significant power reduction at the frequencies even slightly away from the resonant frequency of the harvester [2–4]. Various strategies have been developed to broaden the operational frequency range of piezoelectric harvesters, such as frequency-up conversion [5], multiple resonator array [6], and nonlinearity [7]. Among these, nonlinear bi-stability has exhibited versatile features in harvesting energy from broadband vibrations due to large power output concomitant with the large amplitude snap-through dynamics. Recently, research has demonstrated that nonlinear bi-stable energy harvesters have a higher global performance in terms of power output compared with the linear counterparts and monostable harvesters under the appropriate conditions such that the inter-well vibrations could be activated [8, 9].

Bi-stable piezoelectric vibration energy harvesters are achieved by different mechanisms including mechanical pre-load, magnetic interaction, and laminate composite (residual thermal stress). Extensive reviews on bi-stable energy harvesting could be found in [10,11]. An axially loaded beam was exploited to form a buckled bi-stable piezoelectric vibration energy harvester, which produced up to an order of magnitude more power than the unbuckled case [8]. The clamped-clamped beam with pre-load along the axial direction exhibits the buckled characteristic and bi-stability in response to the transverse excitations, which also has been explored in piezoelectric energy harvesting and showed a wide frequency bandwidth [9, 12]. Harne et al [13] developed a bi-stable energy harvesting device using an inertial mass connected to a translational slide bearing and a pre-compressed spring. For these harvesters, the pre-load leads to the negative stiffness sufficient to overcome the positive stiffness of the system and thus results in bifurcation via buckling. However, exerting a mechanical pre-load to a system usually involves additional constraints. In comparison, magnetic interaction allows a more flexible design of bi-stable systems because of the contactless repulsive or attractive magnetic forces. The repulsive magnetic force between a fixed magnet and the other one at the free end of a cantilever piezoelectric beam injected negative stiffness into the system and thus created a bi-stable harvester [14, 15]. Two tilted magnets and a cantilever beam with another tip magnet were used to create a bi-stable piezoelectric harvester [16]. A magnetically coupled 2-DOF bi-stable energy harvester consisting of two rotary piezoelectric cantilevers with tip magnets was developed for energy harvesting from rotational motions of multiple frequency bands [17]. Bi-stability is also found in laminated composites, where the residual thermal stress difference develops curvatures after the curing procedure from a high temperature to the room temperature due to the various thermal expansion coefficients in different layers [18, 19]. Syta et al [20,21] reported the experimental study on the nonlinear dynamics of a bi-stable piezoelectric laminate plate and examined the modal response using the Fourier spectrum of the time domain voltage responses. Pan et al [22] investigated the influence of the layout of the hybrid symmetric laminates on the bi-stable energy harvesting performance and the dynamics via finite element numerical analysis and experimental validation [23]. Besides, the complicate manufacture process and high cost, laminate composites are sensitive to environmental moisture and temperature, resulting in changes in material properties during long-term service.

This paper proposes a novel bi-stable piezoelectric energy harvester inspired by the rapid shape transition of the Venus flytrap leaves. The bio-inspired design principles of the harvester are elaborated in detail. A cantilever beam is tailored into two sub-beams, whose free ends are constrained by an in-plane pre-displacement to create the bending and twisting curves and to inject mechanical potential energy. Different from the traditional mechanical pre-load method, the proposed bio-inspired bi-stable piezoelectric energy harvester (BBPEH) doesn't need additional constraints to exert the pre-load on the harvester, instead, the pre-load is applied by the interlocking of the free ends of the two sub-beams. The nonlinear dynamics and the energy harvesting performance of the proposed bi-stable piezoelectric energy harvester are studied under different base excitation levels.

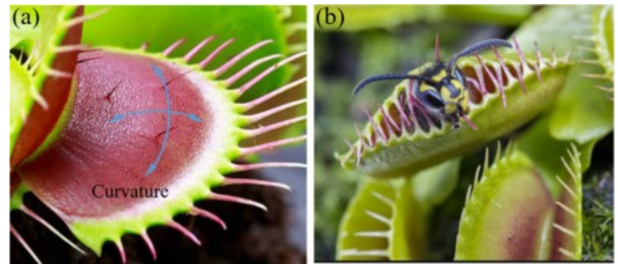

FIGURE 1. Bio-inspired design of the bi-stable piezoelectric energy harvester: (a) first stable state (b) second stable state.

1 Bio-inpired design

The sudden snap-through of a nonlinear bi-stable structure is usually associated with a large energy release, which results in a large power output desired for vibration energy harvesting. A good example of the bi-stable nonlinearity in nature is the Venus flytrap, whose leaves are bi-curved in two directions and have two layers of lopes with local tissues, porous structures, and fluid in between. The leaves will close when the inner layer contracts and outer layer stretches and will open in reverse, as shown in Fig. 1(a) and (b), respectively. Consequently, the shapes of the curved leaves are almost flat at the first stable (open) state and concave at the second stable (close) state [24]. The plant achieves the open state by stretching its leaves back, during which the leaves store potential mechanical energy in the form of elastic energy. The stored energy will be released in the form of hydraulic movement in the porous structures when the leaves are triggered to snap shut. The rapid shape transition from the open state to the closed state as the leaves sense external stimulus is referred to as the snap-through phenomenon which is accompanied by a large energy release. If this snap-through mechanism could be used for energy harvesting, large power output can be achieved due to the concomitant higher energy release. In summary, the knowledge learned from the snap-through mechanism of the Venus flytrap includes: 1) the leaves are bi-curved in two directions, 2) the leaves store potential mechanical energy.

Inspired by the rapid shape transition of the hyperbolic leaves of the Venus flytrap, a novel bi-stable piezoelectric energy harvester is developed in this study to harvest energy from broadband vibrations. The host structure of the proposed BBPEH is tailored from a cantilever beam, as illustrated in Fig. 2 (a), by cutting off the middle strip along the length direction. In this

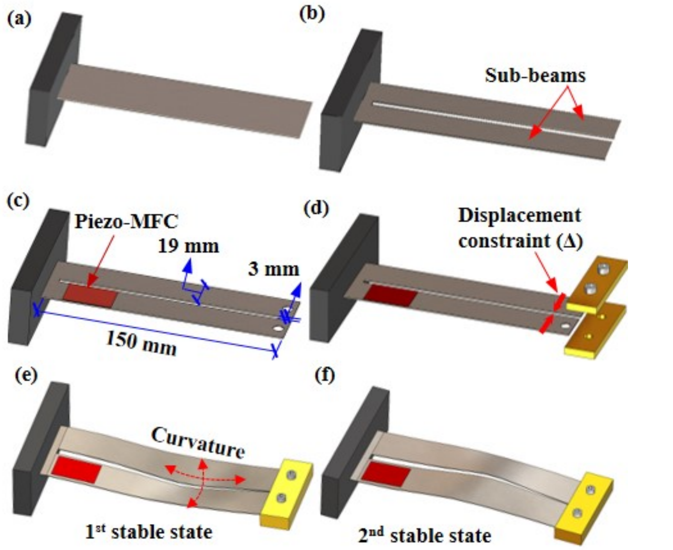

FIGURE 2. Desing of the proposed bio-inspired bi-stable piezoelectric energy harvester.

case, the resultant structure has two sub-beams, as shown in Fig. 2 (b). A piezoelectric transducer is attached on the surface of one of the sub-beams close to the clamped end to covert the strain energy of the vibrating beam into electrical charges. To introduce the two-directional curvature, an in-plane pre-displacement Δ along the width direction of the sub-beams is applied oppositely to the two free ends, which are then constrained by two rigid blocks, as depicted in Fig. 2 (b). These rigid blocks also play the role of tip mass that could tune the local resonant frequency of the nonlinear harvester. This in-plane pre-deformation constraint induces both bending and twisting deformations in the sub-beams and therefore curvatures in both the length and width directions. The deformed structure also stores the potential energy of bending and twisting deformations resulting from the applied pre-displacement constraint, which is analogous to the potential energy in the Venus flytrap. Since the bending and twisting deformations are achievable bidirectionally for the sub-beams, the structure therefore has two stable states, as illustrated in Fig. 2 (c) and (d), respectively.

The proposed BBPEH satisfies the two conditions learned from the snap-through mechanism of the Venus flytrap. When the harvester subjects to base excitations, it will vibrate either locally around one of the stable states (shown in Fig. 2 (c) and (d)) or globally snap through from one stable state to the other. The design takes full advantage of the mutual constraint and balance of the two sub-beam structures to achieve the pre-stress purpose. Compared with traditional bi-stable piezoelectric energy harvesters, the merits of the proposed BBPEH lie in the low-cost, easy manufacturing, and free from the magnetic field. In addition, the quickly snap-through motion between the two stable states can cause high-frequency local vibrations of the sub-beams due to the sudden energy release. This indicates that even under a low-frequency excitation, the sub-beams can locally vibrate at very high-frequencies after the snap-through motion happens. This strategy that converts the low-frequency excitation to a high-frequency vibration is highly desired in energy harvesting to attain a large power output under low-frequency environments, which is usually achieved by frequency up-conversion techniques [25, 26].

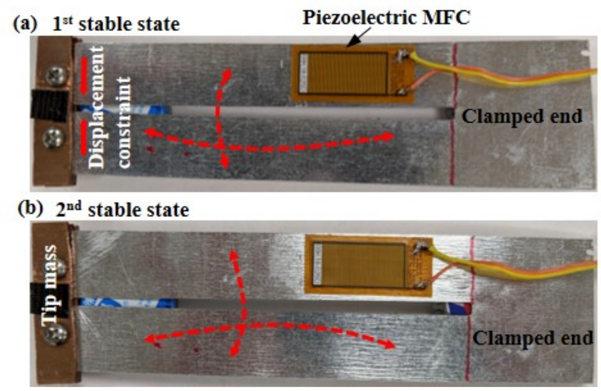

FIGURE 3. The prototype of the proposed bio-inspired bi-stable piezoelectric energy harvester: (a) first stable state, (b) second stable state.

2 Modeling and experimental tests

To verify the concept of the bio-inspired design of the bi-stable piezoelectric vibration energy harvester, a prototype is made of a metal cantilever, piezoelectric macro fiber composite (MFC, M2814-P2, Smart Material Corp.), and two rigid copper blocks. Fig. 3 (a) and (b) show the first and second stable states of the manually manufactured prototype of the BBPEH. The active length and width of the piezoelectric MFC are 28 mm and 14 mm, respectively. The thickness of the beam is 0.381 mm and the other dimensions of the harvester are labeled in Fig. 2 (b).

2.1 Modeling

The dynamics of a bi-stable beam structure with the axial pre-stress can be described by a simplified lumped-mass model with coupled higher-order terms induced by the axial motion. The governing equations of the proposed BBPEH include both the mechanical and electrical equations, which are given as the following [12, 27]

$$\ddot{x}+2\xi\omega_n\dot{x}+\beta(x\dot{x}^2+x^2\ddot{x})+f_{nl}(x)+\theta v+\bar{\theta}x^2v=-\mu\ddot{y} \quad (1)$$

$$C_p\dot{v}+\frac{v}{R}-\theta\dot{x}-\alpha x^2\dot{x}=0 \quad (2)$$

where x and v are the tip displacement of the BBPEH and voltage output across the external resistive load R. The over dot indicates the derivatives with respect to time. ξ is the damping ratio, β and α are the coefficients of the coupled higher-order terms induced by the axial motion, θ and $\bar{\theta}$ are the electromechanical coupling coefficients, μ is the inertia force factor due to the distributed mass of the harvester, $\ddot{y}$ is the base excitation acceleration. $f_{nl} = \frac{\bar{f}_{nl}}{m}$, where $\bar{f}_{nl}$ is the measured nonlinear restoring force and m is the effective mass of the harvester that can be identified from the local natural frequencies and the linear stiffness around the equilibria. C_p = 48 nF is the capacitance of the piezoelectric MFC given in the datasheet.

An experiment was first carried out to measure the nonlinear restoring force $\bar{f}_{nl}$ of the harvester, which characterizes the relationship of the displacement and force using a stander and a ball-screw drive mechanism and a force gauge (Mark-10 M2-2). In the experiment, the clamped end of the BBPEH is fixed to a supporter and the free end is connected to the force gauge with a U-shape adapter and two pins. The two pins clip the free end of the harvester while not hold tightly, in which case the freed end of the BBPEH could move freely in the axial direction as the free end is driven forward and backward by the force gauge. A laser displacement sensor (Micro Epsilon optoNCDT 1302) is used to measure the tip displacement of the harvester, which is also the travel distance of the ball-screw. Experimental results show that the nonlinear restoring force measured when the BBPEH moves from the first stable state to the second stable state is asymmetric to the one measured when the BBPEH moves back from the second stable state to the first stable. This is because of the boundary conditions, imperfect geometry properties, and asymmetrical stress distribution in the harvester. This asymmetry in the nonlinear restoring force which also has been found in the bi-stable composite structure [28] and shallow arch [29] results in the discontinuity of the nonlinear stiffness and the asymmetric potential wells. The fitted nonlinear restoring force functions are given by

$$\bar{f}_{nl}(x) = \begin{cases} f_{r1} = \sum_{i=0}^{6} k_{1i}x^i, 1^{st} \text{ stable state to } 2^{nd} \text{stable state} \\ f_{r2} = \sum_{i=0}^{6} k_{2i}x^i, 2^{nd} \text{ stable state to } 1^{st} \text{stable state} \end{cases} \quad (3)$$

where the coefficients $k_1 = \{k_{1i}, i = 1,2,...,6\} = [1.710, -6.016, -3.052 \times 10^4, -2.816 \times 10^6, -1.335 \times 10^8, -3.363 \times 10^9, -3.510 \times 10^{10}]$, and $k_2 = \{k_{2i}, i = 1,2,...,6\} = [-1.520, 54.48, 1.798 \times 10^4, 7.930 \times 10^6, 1.296 \times 10^8, 4.926 \times 10^9, 7.605 \times 10^{10}]$.

2.2 Experimental setup for dynamic tests

Experiments were conducted to the prototype to validate the design, identify the system parameters, and evaluate the energy harvesting performance of the proposed BBPEH. The experimental setup is shown in Fig. 4, where the harvester was fixed on a VT-600 shaker providing base excitations. The Polytech Laser

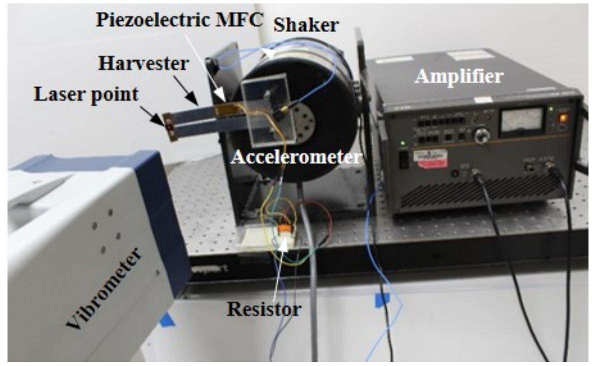

FIGURE 4. Experimental setup of dynamics tests.

vibrometer (Model # PSV-500) was used to measure the tip velocity and record the voltage output of the harvester. The input signal was generated from the laser vibrometer, amplified by an amplifier, and then fed to the shaker. The PCB accelerometer (PCB 356A17) was employed to measure the base excitation acceleration. Frequency sweep experiments were performed firstly with very low excitation levels (amplitudes) to identify the local resonant frequency ω_n under the open circuit and the electromechanical coupling coefficient θ of the harvester at the first stable state. The local vibration resonant frequency of the harvester was found to be ω_n=12.47 Hz at the first stable state. The remaining system parameters were identified from the frequency sweep experiment under a higher excitation level and given as follows: $\xi = 5.6 \times 10^{-3}, \beta = 1.0, \theta = 2.821 \times 10^{-5}, \bar{\theta} = 0.2, \mu = 0.33$, and $\alpha = 6.08 \times 10^{-2}$.

3 Results and discussion

The numerical simulations are performed on the simplified model with the input acceleration excitations measured from experiments. The experimental measurements and simulated results of the frequency sweep at a lower level are plotted in Fig. 5(a) and (b), respectively, including the tip displacements, velocities, and voltages across an external resistive load of R = 180 kΩ. The left column of Fig. 5 plots the upward frequency sweep results, while the right column gives the downward frequency sweep results. The displacement responses in Fig. 5 clearly show the system only oscillates around the first stable state for both the upward and downward frequency sweep, and the voltage responses are small, in particular for the case of the upward frequency sweep. The numerical simulation results in Fig. 5 (b) agree well with the measurements for the small-amplitude intra-well oscillations in Fig. 5 (a). Fig. 6 (a) and (b) plot the experimentally measured and numerically simulated frequency sweep results at a higher excitation level. The snap-through vibrations could be observed from the displacement responses in Fig. 6 (a) and (b) for both the upward and downward

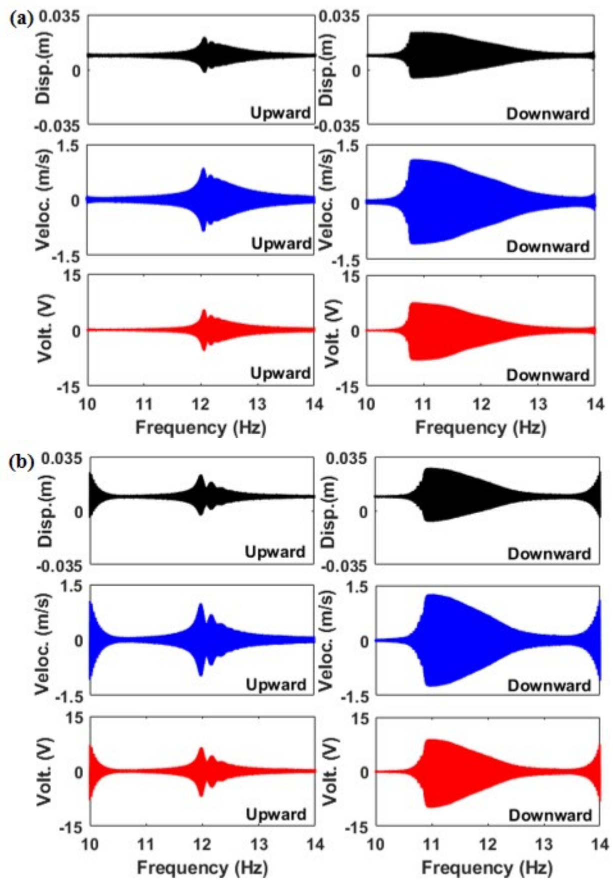

FIGURE 5. Frequency sweep experiment results of intra-well vibrations: (a) experiment, (b) simulation.

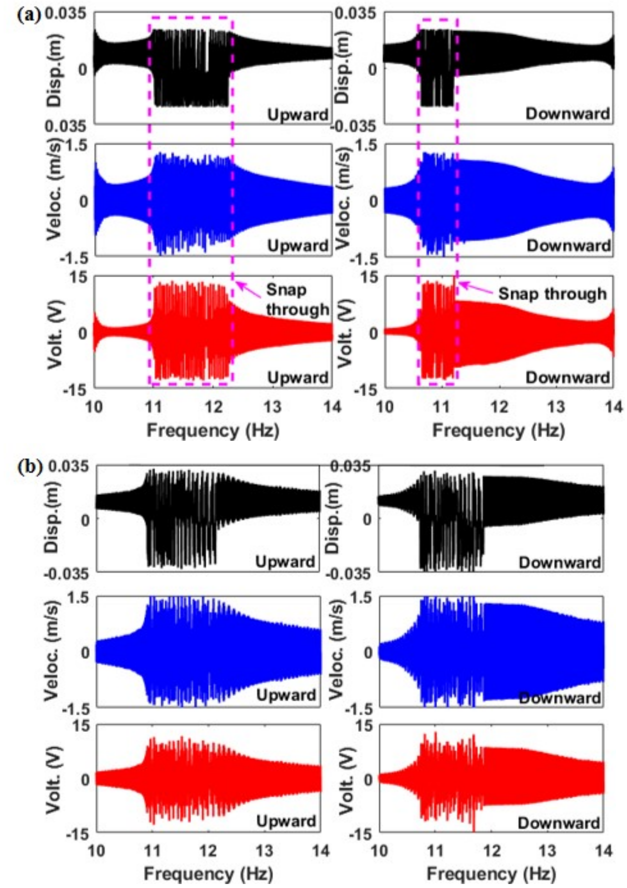

FIGURE 6. Frequency sweep experiment results of inter-well vibrations: (a) experiment, (b) simulation.

frequency sweep, which are accompanied by large voltage responses over the frequency interval of 10.6-12.3 Hz. However, evident discrepancies are observed for the inter-well vibrations from Fig. 6 (a) and (b). Specifically, the simulation results of the downward frequency sweep show a shift in the wider frequency bandwidth (10.8-11.8 Hz) of the inter-well vibrations than the experimental results (10.0-10.9 Hz). These discrepancies are attributed to the model errors and noise in the measured acceleration excitation, especially the error in the measured force-displacement relationship.

To investigate the dynamics of the proposed BBPEH, experiments were also carried out at harmonic base acceleration excitations with a frequency of 12 Hz close to the local resonant frequency and different amplitudes. Fig. 7 (a)-(f) plots the time domain velocity responses of the tip mass and the corresponding power spectrum obtained from FFT analysis for the excitation amplitudes of 0.1 g, 0.6 g, and 4.0 g, respectively. Fig. 7 (a) and (c) indicate that the tip mass experiences an almost perfect periodic motion under the lower excitation levels of 0.1 g and 0.6 g, and the corresponding power was concentrated at the excitation frequency of 12 Hz, as shown in Fig. 7 (b) and (d). However, the weak superharmonic responses due to the nonlinearity were still observed at 24 Hz and 36 Hz under the excitation level of 0.6 g after zooming in the power spectrum, as shown in the inset in Fig. 7 (d). As the excitation amplitude further increases to 4.0 g, the system experiences the snap-through phenomenon and exhibits very strong nonlinear vibrations, as illustrated in Fig. 7 (e). These results also demonstrate that the nonlinear degree of the system increases along with the external excitation level. The power spectrum in Fig. 7 (f) shows more peaks over multiple frequencies in addition to the excitation frequency. Syta et al. [20] defined this type of response with clear and distinct peaks in the power spectrum as the multi-frequency regular snap-through response. The snap-through motion of the harvester could become chaotic at different excitation frequencies and levels. As an example, Fig. 8 presents the velocity response and the power spectrum of the harvester under the excitation level of 4.0 g at 10 Hz, where the power spectrum continuously distributes over a broadband frequency range besides the large-amplitude snap-through

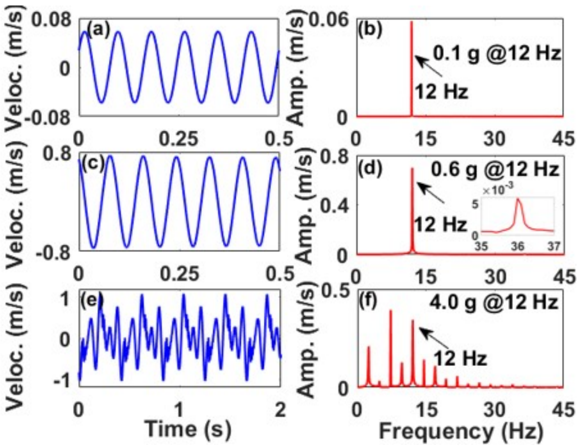

FIGURE 7. Time history and FFT of the tip velocity at the excitation frequency of 12 Hz and amplitudes of 0.1 g (a)-(b), 0.6 g (c)-(d), 4.0 g (e)-(f).

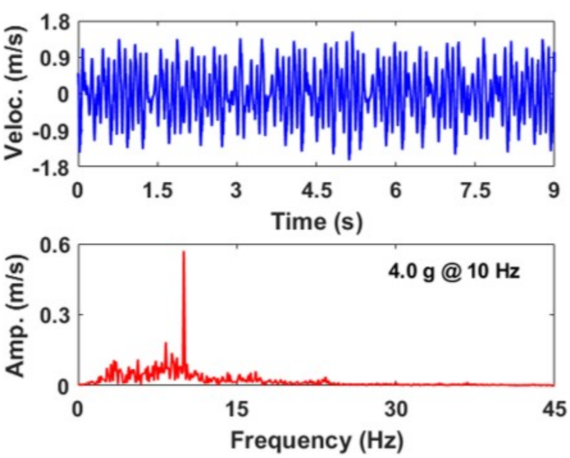

FIGURE 8. Time history and FFT of the tip velocity at the excitation frequency of 10 Hz and amplitudes of 4.0 g

motion at the excitation frequency. This large amplitude nonlinear dynamics between the two potential wells with continuous spectrum over a wideband frequency range was referred to as the twin-well chaotic snap-through motion [30].

The time domain voltage responses of the harvester at the excitation frequency of 12 Hz and different levels of 0.1 g, 0.6 g, and 4.0 g are plotted in Fig. 9 (a)-(f), along with the power spectrum obtained from FFT analysis. At the lower excitation level of 0.1 g, the voltage time series and power spectrum presented in Fig. 9 (a) and (b) exhibit a periodic motion at the single frequency exactly equal to the excitation frequency. Plus, the system also only oscillates in one of the two potential wells under this small excitation level. This vibration is therefore referred to as the single-well period-one motion [30]. As the excitation level increases to 0.6 g, the voltage time series in Fig. 9 (c) shows a period-doubling bifurcation, and the power spectrum in Fig. 9 (d) has two peaks, respectively, at the excitation frequency of 12 Hz and the double of the excitation frequency 24 Hz. The second peak at 24 Hz confirms that the quadratic nonlinearity has a significant contribution to the system dynamics. It should be noted that this periodic intra-well motion with two dominant frequencies is different from the period-two motion referred by M. Panyam et al [30] and S.A. Emam et al [31], where the additional peak of the power spectrum happened at the half instead of the double of the excitation frequency.

The time domain voltage response in Fig. 9 (e) shows the periodic snap-through motion with very high-frequency vibrations at each snap-through phenomenon, which is not observed from the velocity response of the tip mass in Fig. 7 (e). This indicates that the sub-beams of the harvester undergo more complicate local dynamics during the snapping through compared with the tip mass. This high-frequency response is attributed to the local vibrations of the sub-beam, where the piezoelectric MFC transducer is attached. The power spectrum of the voltage response is plotted in Fig. 9 (f), which confirms that the sub-beams experience multiple high-frequency dominated dynamics. The continuously distributed spectrum over the wide frequency range suggests the chaotic motion of the sub-beams during the large amplitude inter-well vibrations. This suggests that the proposed BBPEH could extend the effective frequency range over a quite wide bandwidth aside from the single excitation frequency, and therefore generates more power. It should be mentioned that a much lower external resistor of 8.2 kΩ was used for the inter-well vibration because of the high-frequency local vibrations during snapping through, instead of 180 kΩ used for the case of intra-well vibrations. Nevertheless, the voltage outputs are still much higher than those of the local intra-well vibrations plotted in Fig. 9 (a) and (c) even at a much lower resistive load due to the large amplitude inter-well vibrations.

The energy harvesting performance of the proposed BBPEH is evaluated by the average power outputs for the large-amplitude inter-well vibration. The average power outputs across the external resistive load of $R = 8.20$ kΩ at the excitation levels of 2.0 g, 3.0 g, and 4.0 g and frequency varying from 9 Hz to 14 Hz are presented in Fig. 10. At the excitation level of 2.0 g, the harvester has a significant large power output at the frequency range of 10.5-12.0 Hz because the large amplitude inter-well vibrations are activated. The power output is very small outside of this frequency range due to the small amplitude intra-well dynamics. The frequency bandwidth of the inter-well vibration becomes wider as the excitation level increases to 3.0 g and 4.0 g, which are 10.0-13.0 Hz and 9.5-13.5 Hz, and the average power output also evidently increases over these frequency ranges. The maximum power output is around 0.193 mW at the excitation of 10 Hz and 4.0 g. This wideband feature of the frequency range in which the harvester could achieve snap-through dynam-

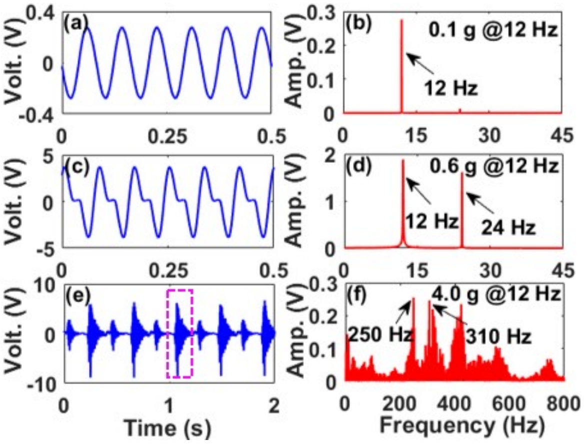

FIGURE 9. Time history and FFT of the voltage output at the excitation frequency of 12 Hz and amplitudes of 0.1 g (a)-(b), 0.6 g (c)-(d), 4.0 g (e)-(f).

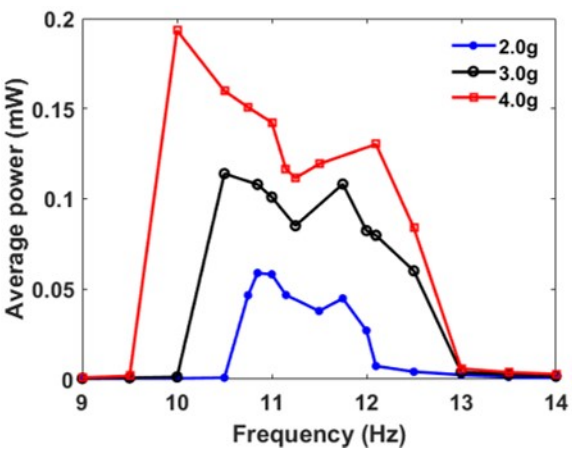

FIGURE 10. Average power outputs of the BBPEH at different excitation levels and frequencies.

ics accompanied by large power outputs is a key design purpose of nonlinear energy harvesters in practice since ambient environment excitations usually contain frequency components over wide frequency broadband.

4 Conclusion

Inspired by the rapid shape transition of the Venus flytrap leaves, a novel bi-stable piezoelectric energy harvester is designed, prototyped, and tested for broadband vibration energy harvesting. Different from traditional ways to achieve bistability using nonlinear magnetic forces or residual stress in laminate composites, the proposed bio-inspired bi-stable piezoelectric energy harvester (BBPH) takes advantage of the mutual self-constraint at the free ends of two cantilever sub-beams with a pre-displacement. This mutual pre-displacement constraint at the free ends bidirectionally curves the two sub-beams due to the bending and twisting deformations and therefore induces mechanical potential energy in the harvester. Both frequency sweep and harmonic experiments are conducted on the prototype to study the nonlinear dynamics and to evaluate the energy harvesting performance. Results show that the sub-beams experience much richer local dynamics with multiple high-frequency vibrations compared with the tip mass even under a single low-frequency harmonic excitation. These local high-frequency vibrations are desirable for high power output. The average power output of the BBPH shows an increasing trend in both the amplitude and frequency bandwidth as the excitation level increases and is high enough to activate the large amplitude inter-well vibration.

ACKNOWLEDGMENT

The authors gratefully acknowledge the financial support from the National Science Foundation (Award Number: 1935951).

REFERENCES

[1] Zhao, L.-C., Zou, H.-X., Yan, G., Liu, F.-R., Tan, T., Wei, K.-X., and Zhang, W.-M., 2019. "Magnetic coupling and flextensional amplification mechanisms for high-robustness ambient wind energy harvesting". *Energy Convers Manage,* ***201***, p. 112166.

[2] Li, Z., Zu, J., and Yang, Z., 2018. "Introducing hinge mechanisms to one compressive-mode piezoelectric energy harvester". *J Renewable Sustainable Energy,* ***10***(3), p. 034704.

[3] Jiang, X.-Y., Zou, H.-X., and Zhang, W.-M., 2017. "Design and analysis of a multi-step piezoelectric energy harvester using buckled beam driven by magnetic excitation". *Energy Convers Manage,* ***145***, pp. 129 – 137.

[4] Qian, F., Zhou, S., and Zuo, L., 2020. "Improving the off-resonance energy harvesting performance using dynamic magnetic preloading". *Acta Mech. Sin.*, pp. 1–11.

[5] Fan, K., Chang, J., Chao, F., and Pedrycz, W., 2015. "Design and development of a multipurpose piezoelectric energy harvester". *Energy Convers Manage,* ***96***, pp. 430 – 439.

[6] Wu, P. H., Chen, Y. J., Li, B. Y., and Shu, Y. C., 2017. "Wideband energy harvesting based on mixed connection of piezoelectric oscillators". *Smart Mater Struct,* ***26***(9), aug, p. 094005.

[7] Daqaq, M. F., Masana, R., Erturk, A., and Dane Quinn, D., 2014. "On the Role of Nonlinearities in Vibratory Energy Harvesting: A Critical Review and Discussion". *Appl Mech Rev,* ***66***(4), 05. 040801.

[8] Cottone, F., Gammaitoni, L., Vocca, H., Ferrari, M., and Ferrari, V., 2012. "Piezoelectric buckled beams for random vibration energy harvesting". *Smart Mater Struct,* ***21***(3), feb, p. 035021.

[9] Andò, B., Baglio, S., Bulsara, A., and Marletta, V., 2014. "A bistable buckled beam based approach for vibrational energy harvesting". *Sens Actuators A,* ***211***, pp. 153 – 161.

[10] Harne, R. L., and Wang, K. W., 2013. "A review of the recent research on vibration energy harvesting via bistable systems". *Smart Mater Struct,* ***22***(2), jan, p. 023001.

[11] Pellegrini, S. P., Tolou, N., Schenk, M., and Herder, J. L., 2013. "Bistable vibration energy harvesters: A review". *J Intell Mater Syst Struct,* ***24***(11), pp. 1303–1312.

[12] Qian, F., Zhou, S., and Zuo, L., 2020. "Approximate solutions and their stability of a broadband piezoelectric energy harvester with a tunable potential function". *Commun Nonlinear Sci Numer Simul,* ***80***, p. 104984.

[13] Harne, R. L., Thota, M., and Wang, K. W., 2013. "Bistable energy harvesting enhancement with an auxiliary linear oscillator". *Smart Mater Struct,* ***22***(12), nov, p. 125028.

[14] Ferrari, M., Ferrari, V., Guizzetti, M., Andò, B., Baglio, S., and Trigona, C., 2010. "Improved energy harvesting from wideband vibrations by nonlinear piezoelectric converters". *Sens Actuators A,* ***162***(2), pp. 425 – 431. Eurosensors XXIII, 2009.

[15] Stanton, S. C., McGehee, C. C., and Mann, B. P., 2010. "Nonlinear dynamics for broadband energy harvesting: Investigation of a bistable piezoelectric inertial generator". *Physica D,* ***239***(10), pp. 640 – 653.

[16] Zhou, S., Cao, J., Erturk, A., and Lin, J., 2013. "Enhanced broadband piezoelectric energy harvesting using rotatable magnets". *Appl Phys Lett,* ***102***(17), p. 173901.

[17] Zou, H.-X., ming Zhang, W., Li, W.-B., Wei, K.-X., Gao, Q.-H., Peng, Z.-K., and Meng, G., 2017. "Design and experimental investigation of a magnetically coupled vibration energy harvester using two inverted piezoelectric cantilever beams for rotational motion". *Energy Convers Manage,* ***148***, pp. 1391 – 1398.

[18] Arrieta, A. F., Delpero, T., Bergamini, A. E., and Ermanni, P., 2013. "Broadband vibration energy harvesting based on cantilevered piezoelectric bi-stable composites". *Appl Phys Lett,* ***102***(17), p. 173904.

[19] Li, Y., Zhou, S., Yang, Z., Guo, T., and Mei, X., 2019. "High-performance low-frequency bistable vibration energy harvesting plate with tip mass blocks". *Energy,* ***180***, pp. 737 – 750.

[20] Syta, A., Bowen, C. R., Kim, H. A., Rysak, A., and Litak, G., 2015. "Experimental analysis of the dynamical response of energy harvesting devices based on bistable laminated plates". *Meccanica,* ***50***(8), Aug, pp. 1961–1970.

[21] Syta, A., Bowen, C. R., Kim, H. A., Rysak, A., and Litak, G., 2016. "Responses of bistable piezoelectric-composite energy harvester by means of recurrences". *Mech Syst Sig Process,* ***76-77***, pp. 823 – 832.

[22] Pan, D., Li, Y., and Dai, F., 2017. "The influence of lay-up design on the performance of bi-stable piezoelectric energy harvester". *Compos Struct,* ***161***, pp. 227 – 236.

[23] Pan, D., Jiang, W., and Dai, F., 2019. "Dynamic analysis of bi-stable hybrid symmetric laminate". *Compos Struct,* ***225***, p. 111158.

[24] Zhang, Z., Chen, D., Wu, H., Bao, Y., and Chai, G., 2016. "Non-contact magnetic driving bioinspired venus flytrap robot based on bistable anti-symmetric cfrp structure". *Compos Struct,* ***135***, pp. 17 – 22.

[25] Fu, H., and Yeatman, E. M., 2019. "Rotational energy harvesting using bi-stability and frequency up-conversion for low-power sensing applications: Theoretical modelling and experimental validation". *Mech Syst Sig Process,* ***125***, pp. 229 – 244.

[26] Fu, H., Sharif-Khodaei, Z., and Aliabadi, F., 2019. "A bio-inspired host-parasite structure for broadband vibration energy harvesting from low-frequency random sources". *Appl Phys Lett,* ***114***(14), p. 143901.

[27] Kim, P., Son, D., and Seok, J., 2016. "Triple-well potential with a uniform depth: Advantageous aspects in designing a multi-stable energy harvester". *Appl Phys Lett,* ***108***(24), p. 243902.

[28] Pan, D., and Dai, F., 2018. "Design and analysis of a broadband vibratory energy harvester using bi-stable piezoelectric composite laminate". *Energy Convers Manage,* ***169***, pp. 149 – 160.

[29] Neville, R. M., Groh, R. M. J., Pirrera, A., and Schenk, M., 2018. "Shape control for experimental continuation". *Phys Rev Lett,* ***120***, Jun, p. 254101.

[30] Panyam, M., Daqaq, M. F., and Emam, S. A., 2018. "Exploiting the subharmonic parametric resonances of a buckled beam for vibratory energy harvesting". *Meccanica,* ***53***(14), Nov, pp. 3545–3564.

[31] Emam, S. A., Hobeck, J., and Inman, D. J., 2019. "Experimental investigation into the nonlinear dynamics of a bistable laminate". *Nonlinear Dyn,* ***95***(4), Mar, pp. 3019–3039.